

GROUPED *B*-SPLINE WINDOWS FOR IMPROVED POWER SPECTRAL DENSITY ESTIMATION

Lucian STANCIU¹, Valentin STANCIU²

*The reduction of the spectral leakage into the side-lobe of a window function is to obtain a more gradual window, with the same length, which generates a lowering of the side lobes amplitude. The usual windows can control these characteristics by using one parameter. To reduce the spectral leakage, a window function in the time domain is used to shape that decrease more gradually toward zero. We propose to use grouped *B*-spline functions to obtain window functions, with increased order of continuity. The power spectral density estimation is optimized by using three control parameters.*

Keywords: spline windows, spectral analysis, frequency leakage, smooth functions, optimal window

1. Introduction

The power spectral estimation implies the determination of the power spectral density (PSD) for different frequency components contained in a signal, by using a finite-length sequence. The windowing of the input signal determines different spectral characteristics from the original continuous-time signal. The behavior due to the windowing is described in the terms of loss of resolution and leakage. It is important the choice of the window to have a good precision for the estimated PSD. We can minimize the spectral leakage [1], [2] by increasing the order of continuity at the boundary of observation windows. The classical window functions can control the resolution or prominent side-lobes by one parameter. A comprehensive comparison of the windows is made based on the computed performance parameters. Windows are weighting functions applied to the finite observation data to reduce the spectral leakage. No window function is perfect for the parameters listed [3], [4], [5].

We propose to use the grouped *B*-spline windows, with three control parameters to solve better this trade-off problem. The proposed windows ensure a high order of continuity in time that has a strong impact on the spectrum of the signal and permits a trade-off between time and frequency resolution.

¹ Prof., Dept. of Telecommunications, University POLITEHNICA of Bucharest, Romania, e-mail: lucians@comm.pub.ro

² PhD student, University POLITEHNICA of Bucharest, Romania, e-mail: svl117@gmail.com

2. Power spectral density estimation

The PSD is defined by the Fourier transform for the autocorrelation function $r_x(k)$ of the sequence $x(n)$

$$P_x(e^{j\omega}) = \sum_{k=-\infty}^{\infty} r_x(k) e^{-j k \omega} \quad (1)$$

It is impossible to use an infinite length signal in practice therefore, will take the Fourier transform of the autocorrelation estimate results in an estimate of the PSD, which is known as the periodogram

$$P_{per}(e^{j\omega}) = \hat{P}(e^{j\omega}) = \sum_{k=-N+1}^{N-1} r_x(k) e^{-j k \omega} \quad (2)$$

where $2N-1$ is the length of the signal window. It is more convenient to write the periodogram directly by using the windowed signal, which is in turn equal to the N point DFT of $x(n)$

$$P_{per}(e^{j\omega}) = \hat{R}(e^{j\omega}) = \frac{1}{N} \left| \sum_{n=0}^{N-1} x(n) e^{-j \omega n} \right|^2 = \frac{1}{N} \left| \sum_{n=-\infty}^{\infty} f_R(n) x(n) e^{-j \omega n} \right|^2 \quad (3)$$

In (3) $f_R(n)$ is a rectangular window defined by:

$$f_R(n) = \begin{cases} 1, & 0 \leq n \leq N-1 \\ 0, & \text{otherwise} \end{cases} \quad (4)$$

In practice, the periodogram will get samples of the spectral estimate using a DFT as $\hat{P}(e^{j2k\pi/N})$. The estimated PSD corresponds to a periodic convolution between the theoretical PSD and the spectrum of a rectangular window with the length of N samples. The finite record length causes a distortion of the estimated spectrum, involving leakage and resolution loss due to windowing [6], [7]. Therefore, we can say that the periodogram method generates the PSD estimate of the given signal.

3. Spectral analysis using grouped B -spline windows

We are interested to use B -spline functions for PSD estimation. There exist an explicit expression for the centered B -spline function of order k :

$$B_k(x) = \sum_{j=0}^{k+1} \frac{(-1)^j}{k!} C_{k+1}^j \left(x + \frac{k+1}{2} - j \right)^k u\left(x + \frac{k+1}{2} - j\right) \quad (5)$$

where $u(x)$ is the unit step function.

Also a recurrence relation can be used:

$$B_k(x) = \left[\left(\frac{k+1}{2} + x \right) B_{k-1} \left(x + \frac{1}{2} \right) + \left(\frac{k+1}{2} - x \right) B_{k-1} \left(x - \frac{1}{2} \right) \right] / k \quad (6)$$

A B -spline of higher order is defined iteratively by convolution:

$$B_k(x) = B_{k-1}(x) * B_0(x) \quad (7)$$

Where:

$$B_0(x) = \begin{cases} 1, & x \in (-1/2, 1/2) \\ 0, & \text{otherwise} \end{cases} \quad (8)$$

The uniform B -spline function of degree k is obtained by using (5). The Fourier transform of $B_k(x)$ is given by

$$BF_k(\omega) = \left(\frac{\sin(\omega/2)}{\omega/2} \right)^{k+1} \quad (9)$$

We are interested to achieve an increased frequency resolution, by grouping three B -spline functions: one of order k and two of order m :

$$BB_{km}(x) = bB_m(ax-g) + B_k(a_1x) + bB_m(ax+g) \quad (10)$$

where a , a_1 , b and g are real coefficients.

Figs. 1 and 2 illustrate the dependence of the grouped ninth order B -splines on the parameters a and a_1 , respectively. Fig. 1 shows the grouped ninth order B -splines for different values of a . The parameters g and a_1 were fixed at $g = 0.263$, $a_1 = 2.475$.

Fig. 2 shows the dependence of the grouped ninth order B -spline on the parameter a_1 . The parameters g and a were fixed at $g = 0.263$, $a = 2.45$. We can see that the parameters a and a_1 give a fine control for an optimum window.

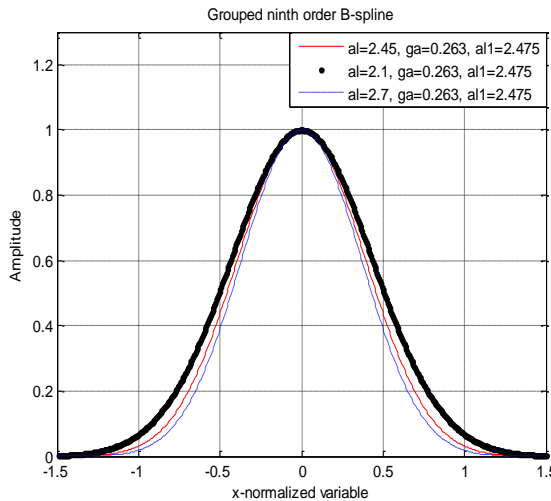


Fig. 1. Grouped ninth order B -spline for different values of a ($a = al$); $g = 0.263$ ($g = ga$); $a_1 = 2.475$ ($a_1 = al1$)

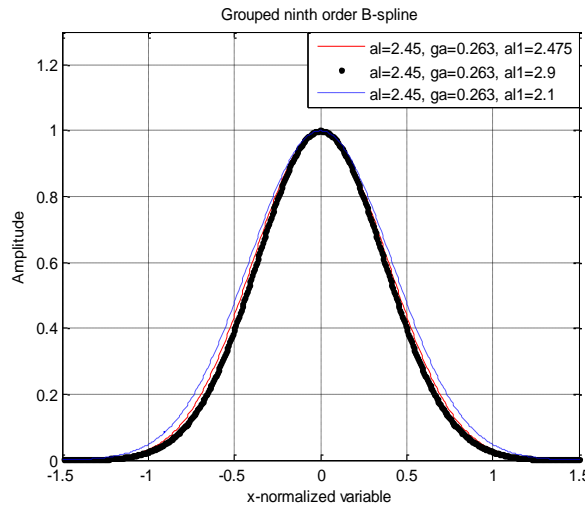


Fig. 2. Grouped ninth order B -spline for different values of a_1 ($a_1 = al1$);
 $a = 2.45$ ($a = al$); $g = 0.263$. ($g = ga$)

Generally, we use the unitary value $BB_{km}(0) = 1$ and the expression for b is:

$$b = \frac{1 - B_k(0)}{B_m(-g) + B_m(g)} \quad (11)$$

The detailed relation for $BB_{km}(x)$ is:

$$BB_{km}(x) = \begin{cases} bB_m(ax + g), & \text{for } -\frac{2g + m + 1}{2a} < x \leq -\frac{k + 1}{2a_1} \\ bB_m(ax + g) + B_k(a_1x), & \text{for } -\frac{k + 1}{2a_1} < x \leq \frac{2g - m - 1}{2a} \\ bB_m(ax + g) + B_k(a_1x) + bB_m(ax - g), & \text{for } \frac{2g - m - 1}{2a} < x \leq \frac{-2g + m + 1}{2a} \\ B_k(a_1x) + bB_m(ax - g), & \text{for } \frac{-2g + m + 1}{2a} < x \leq \frac{k + 1}{2a_1} \\ bB_m(ax - g), & \text{for } \frac{k + 1}{2a_1} < x \leq \frac{2g + m + 1}{2a} \\ 0, & \text{otherwise} \end{cases} \quad (12)$$

The Fourier transform of the grouped B -spline functions from (10), is :

$$BG_k(\omega) = \frac{2b}{|a|} \left[\frac{\sin(\omega/(2a))}{\omega/(2a)} \right]^{m+1} \cos(g\omega) + \frac{1}{|a_1|} \left[\frac{\sin(\omega/(2a_1))}{\omega/(2a_1)} \right]^{k+1} \quad (13)$$

To generate grouped *B*-spline windows, the function given in (12) is uniformly sampled with N samples in the interval $x \in [-p, p]$, where p is $p = \frac{2g+m+1}{2a}$. So we will obtain a discrete causal window for $n = \overline{0, N-1}$.

4. Performance comparison of the grouped *B*-spline windows

We describe various basic parameters of the windows that are useful in choosing an efficient window. Equivalent noise bandwidth is:

$$\eta = \frac{\sum_n f^2(nT)}{\left[\sum_n f(nT) \right]^2} \quad (14)$$

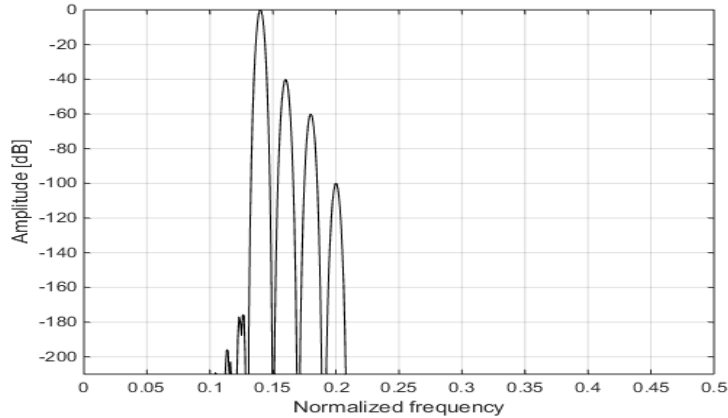


Fig. 3. Spectrum of the signal (18) using the optimum ninth order grouped *B*-spline window ($a=2.45$, $g=0.263$, $a_I=2.475$).

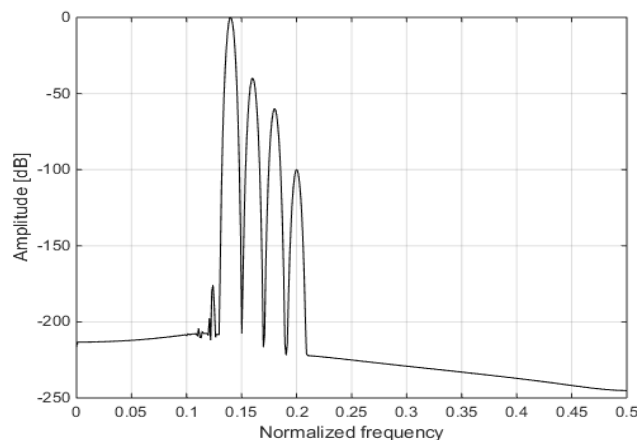


Fig. 4. Spectrum of the signal (18) using the optimum tenth order grouped *B*-spline window ($a=2.455$, $g=0.261$, $a_I=2.477$).

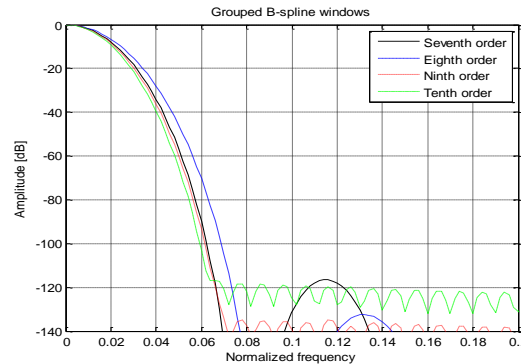


Fig. 5. Frequency response for the optimum seventh, eighth, ninth and tenth order grouped *B*-spline windows ($N=100$).

Table 1

Optimum parameters for grouped *B*-spline windows.

Type	a_1	a	g
Gr. Spl.7	2.37	2.35	0.312
Gr. Spl.8	2.674	2.65	0.282
Gr. Spl.9	2.475	2.45	0.263
Gr. Spl.10	2.477	2.455	0.261

Table 2

Relevant figures of merit for grouped *B*-spline windows.

Type	η	G	$\varepsilon_{\max} [\%]$	SL [dB]
Gr. Spl.7	2.6503	0.2691	-0.0536	-0.4781
Gr. Spl.8	2.8889	0.2467	-0.0453	-0.4029
Gr. Spl.9	2.5549	0.2787	-0.0577	-0.5159
Gr. Spl.10	2.4483	0.2907	-0.0627	-0.5625
Rectangle	1	1	0.5703	3.92
Triangle	1.33	0.5	0.233	1.82
Hamming	1.36	0.54	0.2274	1.78
Blackman	1.73	0.42	0.135	1.1
Kaiser ($\alpha_K=4$)	1.93	0.37	-0.11	0.89

The known bias on spectral amplitudes of the window is defined by the coherent gain factor:

$$G = \frac{1}{N} \sum_n f(nT) \quad (15)$$

Another parameter is the scalloping loss (SL):

$$SL = \frac{\left| \sum_n f(nT) e^{-j\pi/N} \right|}{\sum_n f(nT)} \quad (16)$$

The scalloping loss can be replaced by the maximum relative error ε_{\max} [4]:

$$\varepsilon_{\max} = SL - 1 \quad (17)$$

In (12) the parameters a , a_1 and g are optimized to shape the spectral grouped *B*-spline windows, by minimizing the maximum relative error $|\varepsilon_{\max}|$ for better estimation. We want to present the advantages of the new window functions to estimate the small signals and consider the signal:

$$\begin{aligned} x(n) = & \sin(0.8796n) + 0.01 \sin(1.005n) + 0.001 \sin(1.1309n) + \\ & + 0.00001 \sin(1.2566n) \end{aligned} \quad (18)$$

Fig. 3 shows the spectrum of the signal (18), by using the optimal ninth order grouped *B*-spline window. If we impose $k=m=9$, $BB_9(x) \neq 0$, for $a=a_1=6$, $g=1$ and $x \in (-1, 1)$. By decreasing $a=a_1$, in the first step, and g in the second step, the interferences are minimized. In the next step, a_1 is increased. The optimum values for the three parameters are $a=2.45$, $g=0.263$ and $a_1=2.475$.

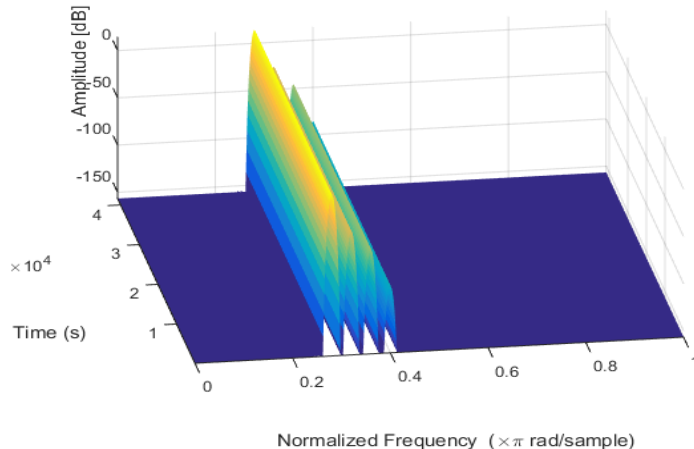


Fig. 6. Spectrogram plot of the signal (18) using the optimum ninth order grouped *B*-spline window

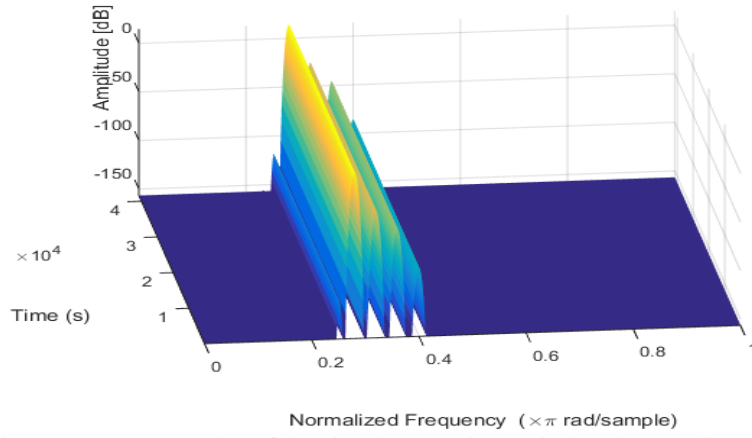


Fig. 7. Spectrogram plot of the signal (18) using a ninth order *B*-spline window.

In the situation $k=m=10$, $BB_{10}(x) \neq 0$, for $a=a_1=6.5$, $g=1$ and $x \in (-1,1)$. In the first step, we decrease the parameters $a=a_1$ and g in the second step, to minimize the interferences. In the final step, a_1 is increased. Finally, we obtain the optimum values $a=2.455$, $g=0.261$ and $a_1=2.477$. By using the optimum tenth order grouped *B*-spline window, the estimated spectrum of the signal (18) is given in Fig. 4. In Fig. 5 are showed the frequency representations for the optimum seventh, eighth, ninth and tenth order grouped *B*-spline windows.

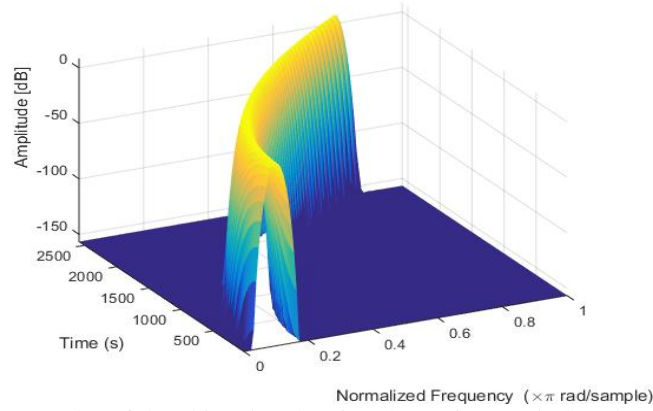


Fig. 8. Spectrogram plot of the chirp signal using the optimum ninth order grouped *B*-spline window.

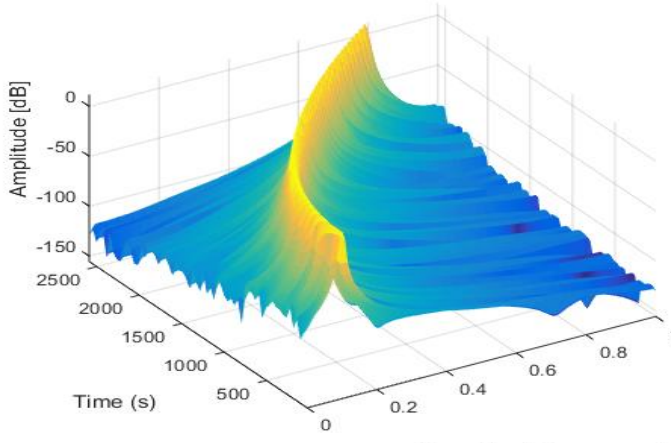


Fig. 9. Spectrogram plot of the chirp signal using Hanning window.

Fig. 6 illustrates the spectrogram plot for the signal (18), by using optimal ninth order grouped B -spline window. By comparison, Fig. 7 shows the spectrogram plot for the signal (18), by using the ninth order B -spline window. The same comparative presentation is made, for the optimum ninth order grouped B -spline window, in Fig. 8, respectively for Hanning window in Fig. 9, for the spectrograms using chirp signal with the quadratic form variation of the signal frequency. We observe that the spectral leakage rapidly decreases for the optimum ninth order grouped B -spline windows.

Fig. 10 shows the spectrogram using chirp signal with the quadratic form variation of the signal frequency, for the optimum tenth order grouped B -spline window.

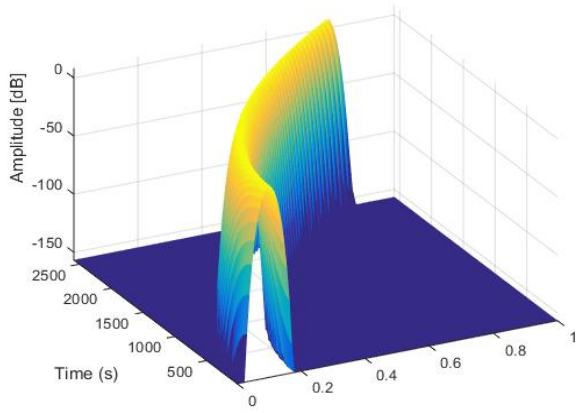


Fig. 10. Spectrogram plot of the chirp signal using the optimum tenth order grouped B -spline window.

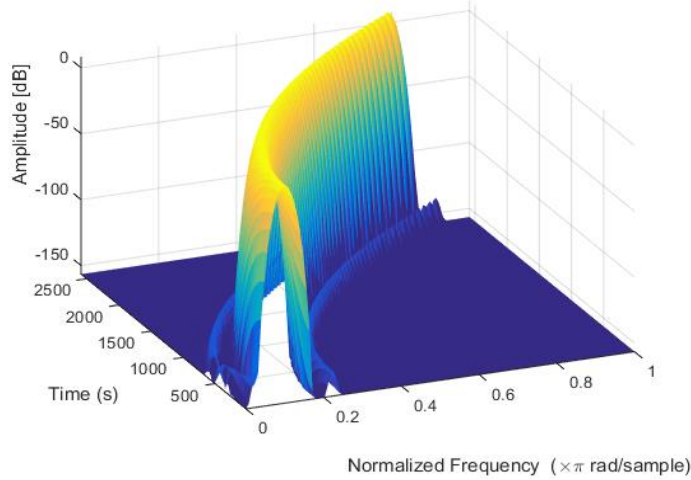


Fig. 11. Spectrogram plot of the chirp signal using the tenth order B -spline.

By comparison, Fig. 11 shows the spectrogram using chirp signal with the quadratic form variation of the signal frequency, by using the tenth order B -spline window.

Table 1 gives the optimum parameters for grouped B -spline windows, of seventh to tenth order. The important figures of merit, for relevant grouped B -spline windows and other windows are summarized in Table 2.

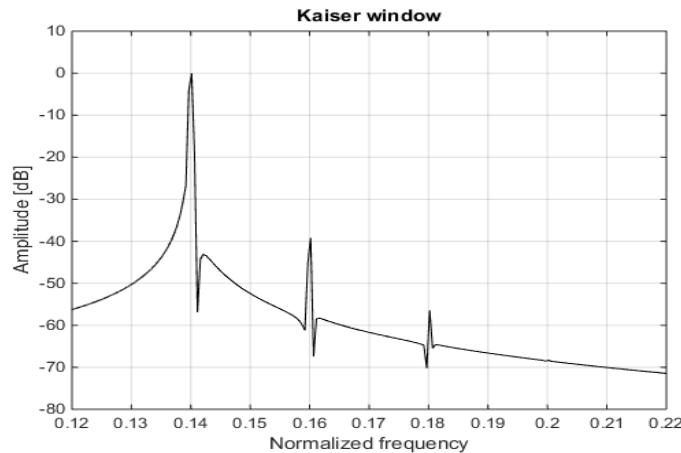


Fig. 12. Spectrum of the signal (18) using Kaiser window ($\alpha_k = 4.5$).

Fig. 12 plots the estimated spectrum for the signal (18), using Kaiser window ($\alpha_k = 4.5$).

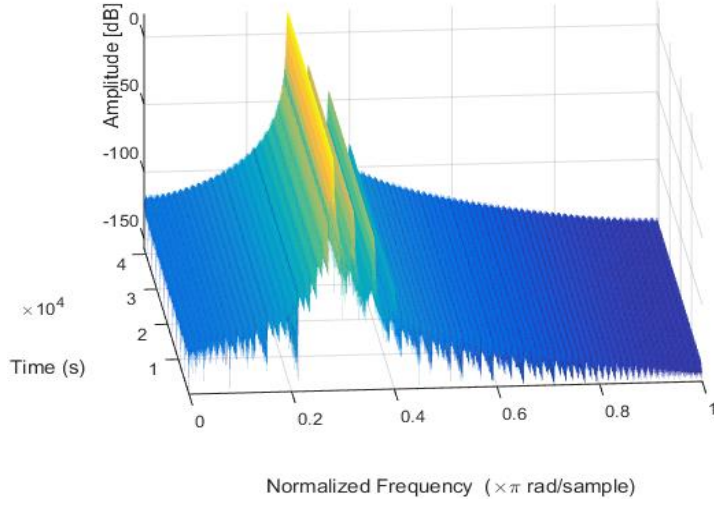


Fig. 13. Spectrum of the signal (18) using Hanning window.

Fig. 13 illustrates the estimation for the signal (18), using Hanning window. In spectral analysis, the side lobes cause smearing or spreading of energy, while the main lobe is responsible for appropriate smoothing effects.

These last results demonstrate the efficacy of the grouped *B*-spline windows exposed, in estimation of small signals, by comparing with other windows.

5. Conclusions

The spectral window does not exhibit side lobes and is as narrow in frequency as possible. The choice of a time-limited window is important for improving the accuracy of the harmonic amplitude. The resolution is sufficient, and the leakage is small, if the main lobe is narrow and the side lobes are low and decrease rapidly, with increasing distance from the main lobe. In this paper, we presented an approach for the construction of the grouped *B*-spline windows. These new windows contain three design parameters that can be used to solve the trade-off problem, to have fast side lobe decay and maximized efficiency for small signal detection. The reduction of leakage is inevitably accompanied by a further loss of resolution, which is related to main lobe width into the side-lobe of a window function. We have tested the spectral effects of these new more gradual window functions in harmonic signal analysis.

The presented applications demonstrate that the grouped *B*-spline windows ensure the possibility of a trade-off between resolution and leakage, by detecting the small signals.

R E F E R E N C E S

- [1] *S. Vaseghi*, Advanced Digital Signal Processing and Noise Reduction, John Wiley and Son, 2008.
- [2] *Yixin Yang, Yahao Zhang, and Long Yang*, “Wideband sparse spatial spectrum estimation using matrix filter with nulling in a strong interference environment”, Statistical The Journal of the Acoustical Society of America 143, 3891 (2018).
- [3] *Adrian Steffens, Patrick Rebentrost, Iman Marvian, Jens Eisert and Seth Lloyd*, “ An efficient quantum algorithm for spectral estimation”, New Journal of Physics, Volume 19, March 2017.
- [4] *L. Stanciu, C. Stanciu, V. Stanciu*, “Optimal Grouped B-Spline for Power Spectral Density Estimation”, ISETC 2014, November 14-15, pp. 333-336, Timisoara, Romania.
- [5] *I. S. Reljin, B. D. Reljin, and V. D. Papic*, “Extremely flat-top windows for harmonic analysis”, Instrumentation and Measurement, IEEE Transactions on, vol. 56, no. 3, pp. 1025–1041, June 2007.
- [6] *Tae Hyun Yoon and Eon Kyeong Joo*, “Butterworth Window for Power Spectral Density Estimation”, ETRI Journal, vol. 31, nr. 3, pp. 292-297, June 2009.
- [7] *L. Stanciu, C. Stanciu, V. Stanciu*, “Smooth Frequency Response Digital Audio Equalizers with Small Ringing Impulse Response”, Revue Roumaine des Sciences Techniques-Serie Electrotechnique et Energetique, pp. 416-425, no. 4, 2015.